Electronic Supplementary Material (ESI) for Dalton Transactions.

"The cation-dependent structural, magnetic and optical properties in a family of hypophosphite hybrid perovskites"

by Mirosław Mączka et al.

e-mail: m.maczka@intibs.pl

Table S1. Experimental details.

For all structures: monoclinic, $\boldsymbol{P2_1/n}$, $\boldsymbol{Z}$ = 4. Experiments were carried out at 295 K with Mo $K\alpha$ radiation using a Xcalibur, Atlas. Absorption was corrected for by multi-scan methods, *CrysAlis PRO* 1.171.38.41 (Rigaku Oxford Diffraction, 2015) Empirical absorption correction using spherical harmonics, implemented in SCALE3 ABSPACK scaling algorithm. Refinement was on 157 parameters. H atoms were treated by a mixture of independent and constrained refinement.

	[Pyr]Mn(H_2POO)$_3$	[EtA]Mn(H_2POO)$_3$
Crystal data		
Chemical formula	$C_4H_{16}MnNO_6P_3$	$C_2H_{14}MnNO_7P_3$
M_r	322.03	311.99
a, b, c (Å)	9.7325 (3), 9.1882 (3), 13.4223 (4)	9.4250 (4), 8.8692 (3), 13.4809 (6)
β (°)	91.018 (3)	93.142 (4)
V (Å^3)	1200.09 (6)	1125.20 (8)
μ (mm^{-1})	1.51	1.61
Crystal size (mm)	0.21 × 0.13 × 0.06	0.18 × 0.14 × 0.05
Data collection		
T_{min}, T_{max}	0.960, 1.000	0.953, 1.000
No. of measured, independent and observed [$I > 2\sigma(I)$] reflections	15018, 2973, 2595	12768, 2774, 2303
R_{int}	0.022	0.026
$(\sin \theta/\lambda)_{max}$ (Å^{-1})	0.688	0.694
Refinement		
$R[F^2 > 2\sigma(F^2)]$, $wR(F^2)$, S	0.025, 0.063, 1.05	0.028, 0.069, 1.05
No. of reflections	2973	2774
No. of restraints	0	6
$\Delta\rangle_{max}$, $\Delta\rangle_{min}$ (e Å^{-3})	0.31, -0.47	0.42, -0.32

Computer programs: *CrysAlis PRO* 1.171.38.41 (Rigaku OD, 2015), *SHELXT* 2018/2 (Sheldrick, 2018), *SHELXT* 2014/5 (Sheldrick, 2014), *SHELXL2018*/3 (Sheldrick, 2018).

Table S2. Selected geometric parameters (Å, º).

[Pyr]Mn(H_2POO)$_3$			
Mn1—O5	2.1621 (12)	P1—O6	1.4894 (13)
Mn1—O5^{i}	2.1621 (12)	P1—O1	1.5001 (12)
Mn1—O4	2.1866 (12)	P2—O4	1.4899 (13)
Mn1—O4^{i}	2.1866 (12)	P2—O3	1.4930 (13)
Mn1—O1^{ii}	2.1977 (11)	P3—O5	1.4728 (13)
Mn1—O1^{iii}	2.1977 (11)	P3—O2	1.4943 (13)
Mn2—O6^{iv}	2.1615 (12)	N1—C1	1.500 (2)
Mn2—O6	2.1615 (12)	N1—C2	1.505 (2)
Mn2—O3^{iv}	2.1718 (11)	C1—C3	1.510 (3)
Mn2—O3	2.1718 (11)	C2—C4	1.507 (3)
Mn2—O2^{v}	2.2118 (12)	C3—C4	1.520 (3)
Mn2—O2^{vi}	2.2118 (12)		
O5—Mn1—O5^{i}	180.0	O6—Mn2—O2^{v}	87.52 (6)
O5—Mn1—O4	89.30 (5)	O3^{iv}—Mn2—O2^{v}	90.93 (5)
O5^{i}—Mn1—O4	90.70 (5)	O3—Mn2—O2^{v}	89.07 (5)
O5—Mn1—O4^{i}	90.70 (5)	O6^{iv}—Mn2—O2^{vi}	87.52 (6)
O5^{i}—Mn1—O4^{i}	89.30 (5)	O6—Mn2—O2^{vi}	92.48 (6)
O4—Mn1—O4^{i}	180.0	O3^{iv}—Mn2—O2^{vi}	89.07 (5)
O5—Mn1—O1^{ii}	90.85 (5)	O3—Mn2—O2^{vi}	90.93 (5)
O5^{i}—Mn1—O1^{ii}	89.15 (5)	O2^{v}—Mn2—O2^{vi}	180.0
O4—Mn1—O1^{ii}	91.32 (5)	O6—P1—O1	115.18 (7)
O4^{i}—Mn1—O1^{ii}	88.68 (5)	O4—P2—O3	118.33 (8)
O5—Mn1—O1^{iii}	89.15 (5)	O5—P3—O2	118.46 (8)
O5^{i}—Mn1—O1^{iii}	90.85 (5)	P1—O1—Mn1^{vii}	129.87 (7)
O4—Mn1—O1^{iii}	88.68 (5)	P3—O2—Mn2^{viii}	134.53 (8)
O4^{i}—Mn1—O1^{iii}	91.32 (5)	P2—O3—Mn2	137.03 (8)
O1^{ii}—Mn1—O1^{iii}	180.0	P2—O4—Mn1	132.54 (8)
O6^{iv}—Mn2—O6	180.0	P3—O5—Mn1	166.25 (10)
O6^{iv}—Mn2—O3^{iv}	90.22 (5)	P1—O6—Mn2	133.97 (8)
O6—Mn2—O3^{iv}	89.78 (5)	C1—N1—C2	108.22 (13)
O6^{iv}—Mn2—O3	89.78 (5)	N1—C1—C3	103.77 (14)
O6—Mn2—O3	90.22 (5)	N1—C2—C4	105.00 (15)
O3^{iv}—Mn2—O3	180.0	C1—C3—C4	103.10 (16)
O6^{iv}—Mn2—O2^{v}	92.48 (6)	C2—C4—C3	103.11 (16)

[EtA]Mn(H_2POO)$_3$			
Mn1—O1^{iv}	2.1798 (13)	Mn2—O5^{i}	2.1512 (15)
Mn1—O1	2.1798 (13)	P1—O1	1.5027 (14)
Mn1—O2^{iv}	2.1889 (13)	P1—O3	1.5035 (14)
Mn1—O2	2.1888 (13)	P3—O5	1.4777 (16)
Mn1—O6^{ix}	2.1881 (14)	P3—O6	1.5011 (15)
Mn1—O6^{x}	2.1881 (14)	P21—O2	1.4857 (17)
Mn2—O3^{xi}	2.2043 (12)	P21—O4	1.4710 (18)
Mn2—O3^{v}	2.2043 (12)	O1A—C1	1.419 (3)
Mn2—O4^{i}	2.1565 (14)	N1—C2	1.481 (3)
Mn2—O4	2.1565 (14)	C2—C1	1.505 (3)
Mn2—O5	2.1511 (15)		
O1^{iv}—Mn1—O1	180.0	O5^{i}—Mn2—O3^{xi}	88.50 (6)
O1^{iv}—Mn1—O2^{iv}	94.65 (6)	O5^{i}—Mn2—O3^{v}	91.50 (6)
O1—Mn1—O2^{iv}	85.35 (6)	O5—Mn2—O3^{xi}	91.50 (6)
O1^{iv}—Mn1—O2	85.35 (6)	O5—Mn2—O4^{i}	86.38 (6)
O1—Mn1—O2	94.65 (6)	O5^{i}—Mn2—O4	86.38 (6)
O1^{iv}—Mn1—O6^{ix}	89.36 (5)	O5—Mn2—O4	93.62 (6)
O1^{iv}—Mn1—O6^{x}	90.64 (5)	O5^{i}—Mn2—O4^{i}	93.62 (6)
O1—Mn1—O6^{x}	89.36 (5)	O5—Mn2—O5^{i}	180.00 (8)
O1—Mn1—O6^{ix}	90.64 (5)	O1—P1—O3	116.28 (8)
O2—Mn1—O2^{iv}	180.0	O5—P3—O6	115.51 (9)
O6^{x}—Mn1—O2^{iv}	90.55 (6)	O4—P22—O2	123.3 (5)
O6^{ix}—Mn1—O2	90.54 (6)	P1—O1—Mn1	125.62 (8)
O6^{ix}—Mn1—O2^{iv}	89.45 (6)	P21—O2—Mn1	139.05 (12)
O6^{x}—Mn1—O2	89.46 (6)	P22—O2—Mn1	147.1 (3)
O6^{ix}—Mn1—O6^{x}	180.0	P1—O3—Mn2^{xii}	119.96 (7)
O3^{v}—Mn2—O3^{xi}	180.0	P21—O4—Mn2	146.63 (14)
O4^{i}—Mn2—O3^{xi}	91.76 (5)	P22—O4—Mn2	164.8 (4)
O4—Mn2—O3^{xi}	88.24 (5)	P3—O5—Mn2	135.75 (10)
O4^{i}—Mn2—O3^{v}	88.24 (5)	P3—O6—Mn1^{xiii}	133.17 (9)
O4—Mn2—O3^{v}	91.76 (5)	O1A—C1—C2	112.77 (18)
O4^{i}—Mn2—O4	180.0	N1—C2—C1	112.82 (17)
O5—Mn2—O3^{v}	88.50 (6)		

Symmetry code(s): (i) -*x*+1, -*y*+1, -*z*+1; (ii) -*x*+1/2, *y*-1/2, -*z*+3/2; (iii) *x*+1/2, -*y*+3/2, *z*-1/2; (iv) -*x*, -*y*+2, -*z*+1; (v) -*x*+1, -*y*+2, -*z*+1; (vi) *x*-1, *y*, *z*; (vii) -*x*+1/2, *y*+1/2, -*z*+3/2; (viii) *x*+1, *y*, *z*; (ix) *x*-1/2, -*y*+3/2, *z*+1/2; (x) -*x*+1/2, *y*+1/2, -*z*+1/2; (xi) *x*, *y*-1, *z*; (xii) *x*, *y*+1, *z*; (xiii) -*x*+1/2, *y*-1/2, -*z*+1/2.

Table S3. Selected hydrogen-bond parameters.

D—H···*A*	*D*—H (Å)	H···*A* (Å)	*D*···*A* (Å)	*D*—H···*A* (°)
[Pyr]Mn(H_2POO)$_3$				
N1—H1···O1	0.89	1.93	2.8069 (19)	166.9
N1—H2···O2^{i}	0.89	2.10	2.8665 (19)	144.3
[EtA]Mn(H_2POO)$_3$				
O1A—H1A···O6	0.74 (2)	2.03 (2)	2.766 (2)	174 (3)
N1—H1C···O3^{ii}	0.89	1.95	2.828 (2)	167.1
N1—H1D···O1^{iii}	0.89	2.11	2.942 (2)	156.1
N1—H1D···O2^{iv}	0.89	2.54	3.123 (2)	123.9
N1—H1E···O1A^{v}	0.89	2.12	2.999 (2)	169.2

Symmetry code(s): (i) *x*-1/2, -*y*+3/2, *z*+1/2; (ii) *x*+1/2, -*y*+3/2, *z*-1/2; (iii) -*x*+1/2, *y*-3/2, -*z*+1/2; (iv) *x*+1/2, -*y*+1/2, *z*-1/2; (v) -*x*+3/2, *y*-1/2, -*z*+1/2.

Table S4. Comparison of distortion factors (δ, σ, Δ), Mn-Mn and Mn-O distances, unit cell volumes per formula unit (V/Z), tolerance factors (TF), Mn-O-P angles, Neel temperatures (T_N) and PL band positions for all manganese hypophosphite simple perovskites at room temperature (except of triazolium analogue for which magnetic and optical properties are not known). For $[GUA]Mn(H_2POO)_3$, data correspond to triclinic phase.

Cation (ionic size in pm)	TF	V/Z (Å^3)	δ (%)	σ(deg.^{2})	Δ(Å) 10^{-5}	Mn···Mn (Å) (average)	Mn-O (Å) average	Mn-O-P (º) (average)	T_N (K)	PL (nm)
FA (253)	0.86	251.4	10.6	3.3	0.09	6.35-6.89 (6.51)	2.194	134.94-143.33 (138.09)	2.4	656
IM (258)	0.87	283.0	1.35	9.1 14.5	7.3 7.1	6.25-6.79 (6.61)	2.181 2.173	128.99-156.3 (135.59)	5.0	646
MHy (264)	0.88	269.4	0.44	8.7	3.0	6.38-6.65 (6.48)	2.1760	127.37-156.35 (138.23)	6.5	686
DMA (272)	0.90	296.0	0.17	4.1 8.9 9.1	3.1 7.5 2.9	6.63-6.71 (6.67)	2.171 2.165 2.162	130.81-153.5 (139.25)	3.4	668
GUA (278)	0.91	280.4	0.5	2.3	32.0	6.52-6.60 (6.56)	2.188	126.93-141.23 (132.40)	6.5	?
Pyr (320)	1.01	300.0	0.18	1.1 2.6	4.6 9.9	6.69-6.71 (6.70)	2.182 2.182	129.87-166.25 (139.03)	6.0	677
EtA (344)	1.06	281.3	0.39	6.7 8.1	12.1 0.4	6.47-6.74 (6.56)	2.171 2.186	119.96-164.80 (138.69)	7.0	689

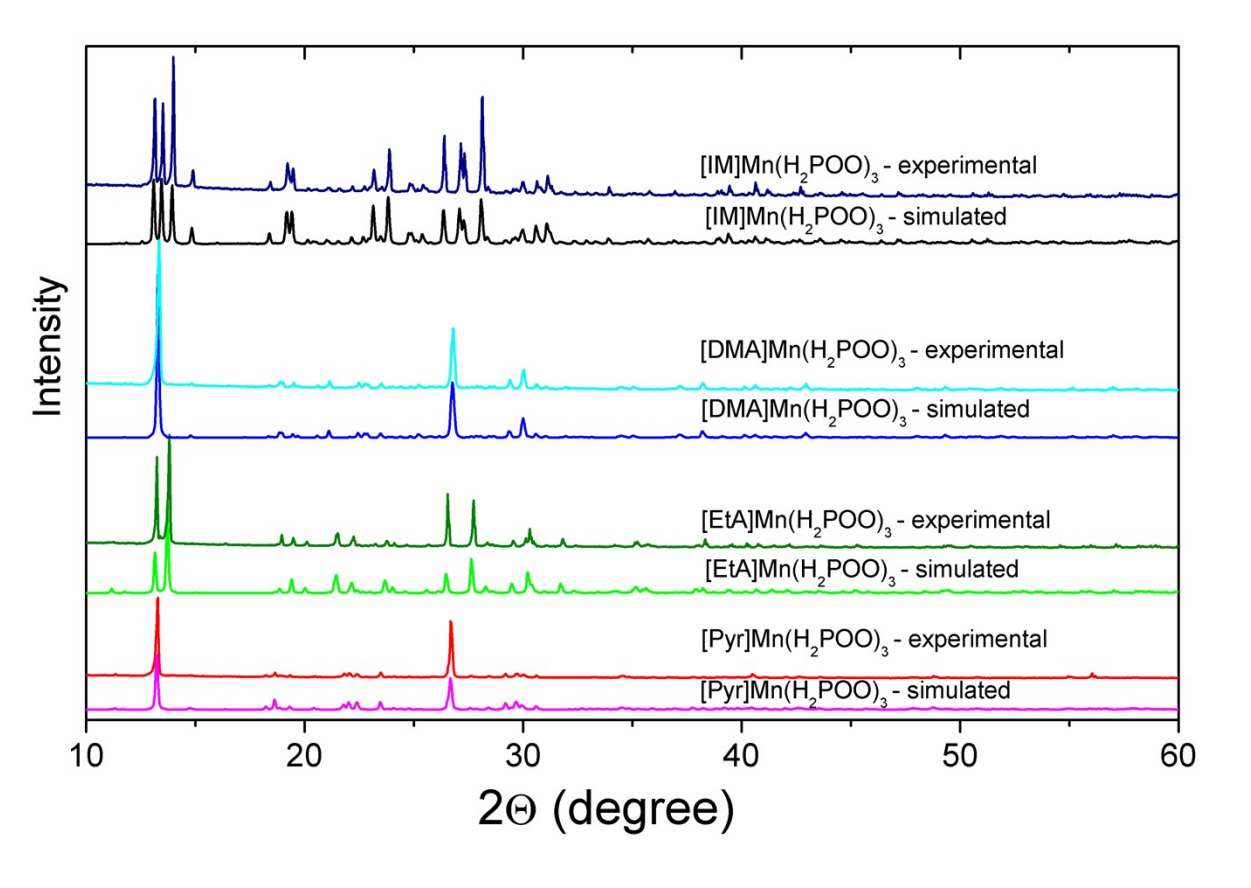

Figure S1. Experimental XRD patterns of the studied compounds together with the calculated ones based on the RT crystal structures.

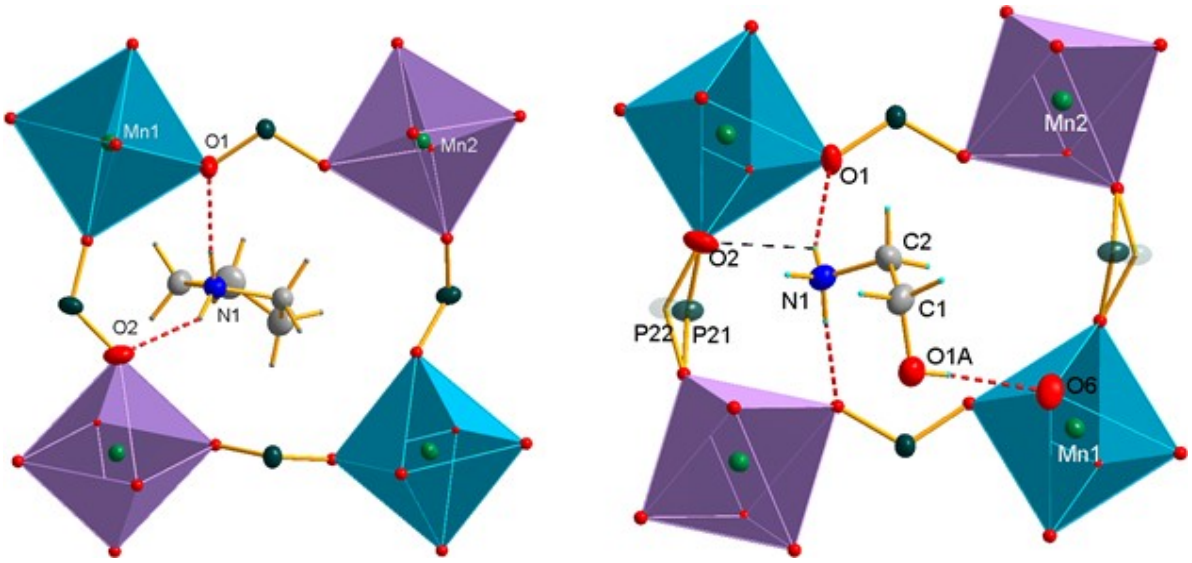

Figure S2. Atom numbering scheme and H-bonds in Pyr (left) and EtA (right) Mn-hypophosphites.

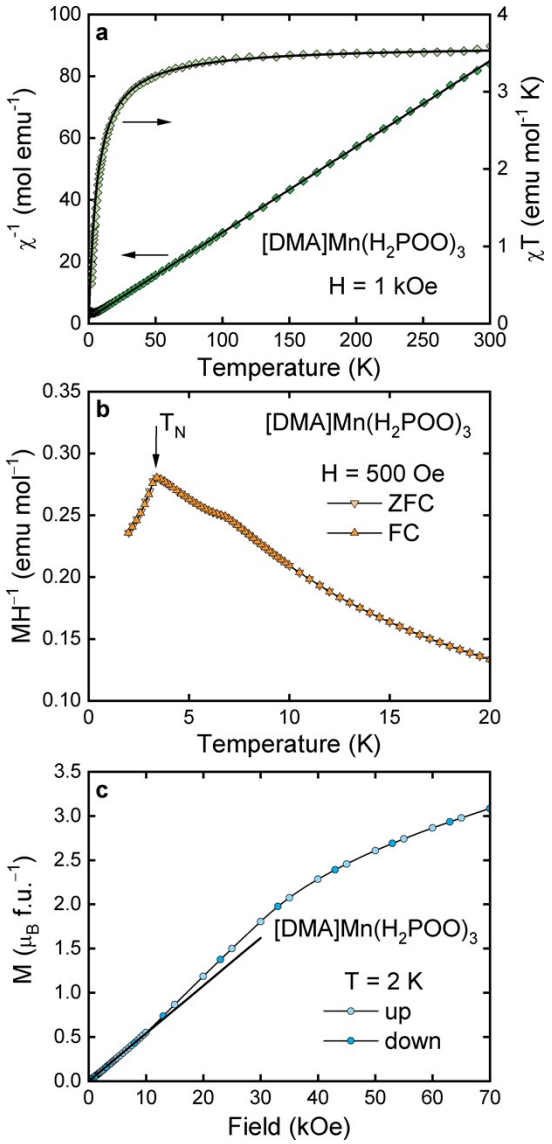

Figure S3. (a) Temperature dependence of inverse DC magnetic susceptibility χ^{-1} (left axis) and a product χT (right axis) of [DMA]Mn(H_2POO)$_3$ measured in constant magnetic field H; thick solid lines are a fit of the Curie-Weiss law to the experimental data (for details see the text). (b) LT magnetization M divided by magnetic field H measured in the ZFC and FC regimes (bright and dark symbols, respectively); the arrow marks the Néel temperature T_N. (c) Magnetization M (expressed as a magnetic moment per formula unit) as a function of increasing and decreasing field H (bright and dark symbols, respectively); the solid line shows linear behavior of M(H) in low fields.

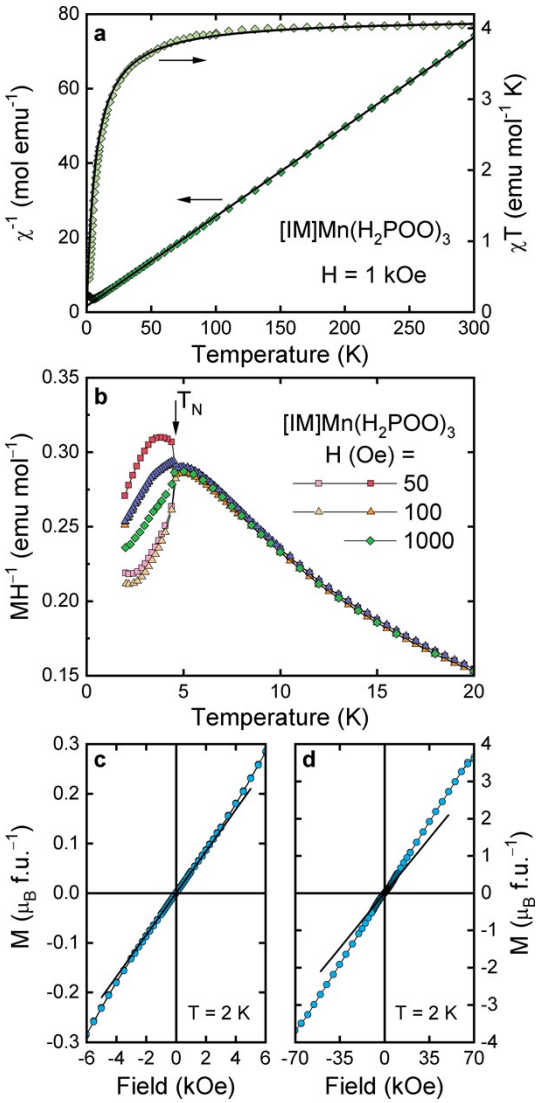

Figure S4. (a) χ^{-1}(T) (left axis) and χT(T) (right axis) of [IM]Mn($H_2POO)_3$; thick solid lines are the Curie-Weiss fit (for details see the text). (b) MH^{-1}(T) with the ordering temperature T_N marked by an arrow, measured in the ZFC and FC regimes (bright and dark symbols, respectively). (c,d) M measured as a function of increasing and decreasing field (bright and dark symbols, respectively) and plotted in two different field ranges; the solid lines show linear part of M(H).

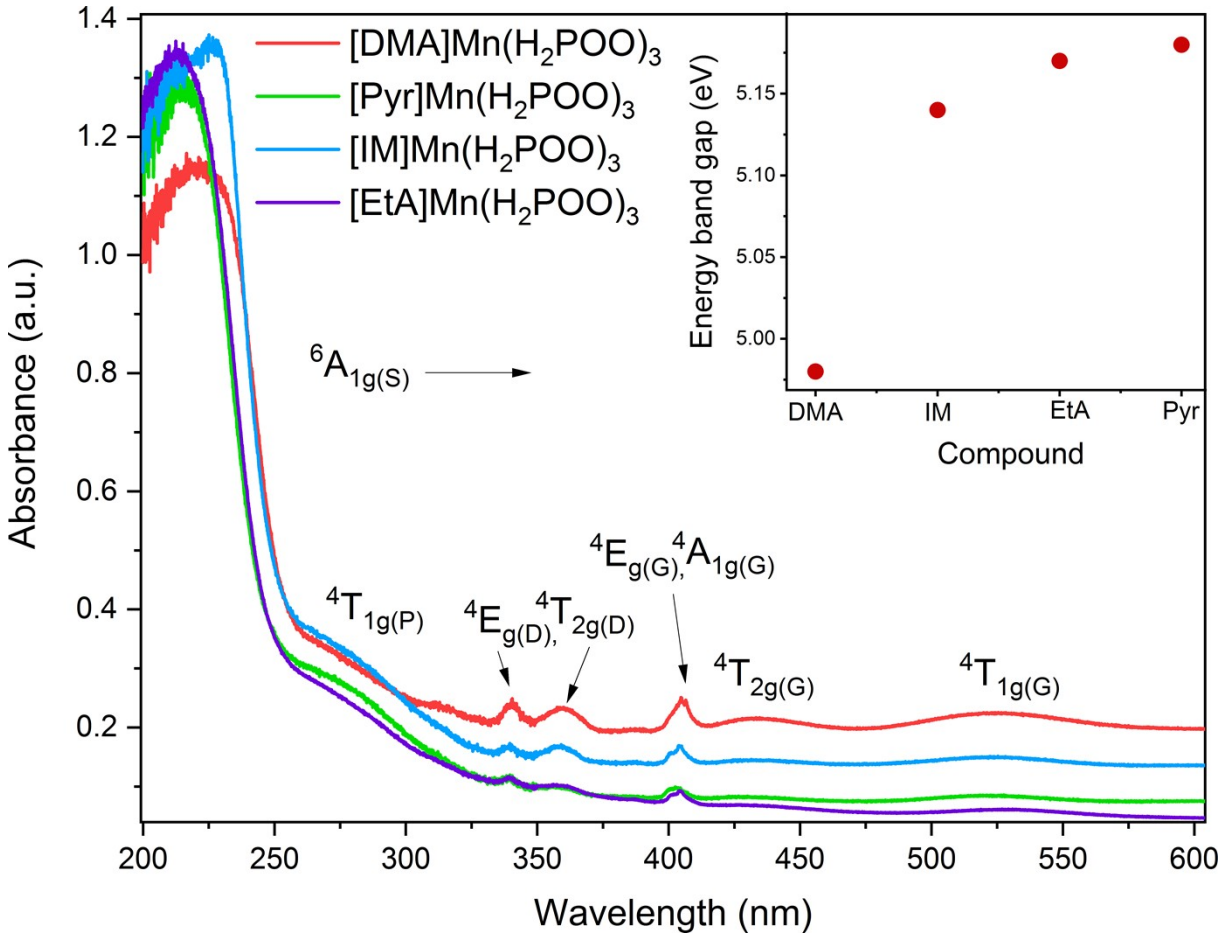

Figure S5. Room temperature absorption spectra of the investigated hypophosphite compounds with assigned Mn^{2+} absorption bands. The inset shows the energy band gap values (E_g) of the investigated compounds.

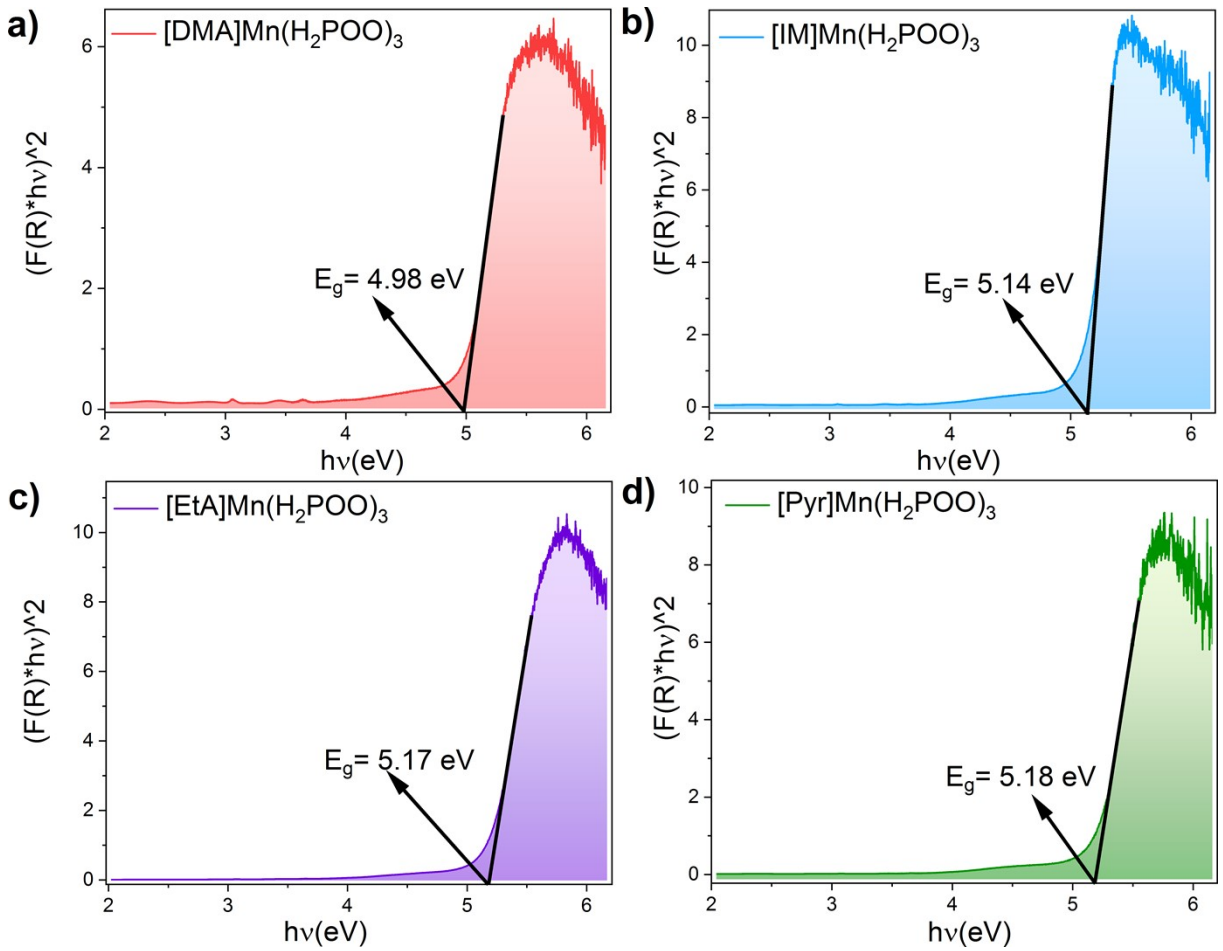

Figure S6. The energy band gap of $[DMA]Mn(H_2POO)_3$ (a) $[IM]Mn(H_2POO)_3$ (b), $[EtA]Mn(H_2POO)_3$ (c), and $[Pyr]Mn(H_2POO)_3$ (d) determined using Kubelka-Munk relation.

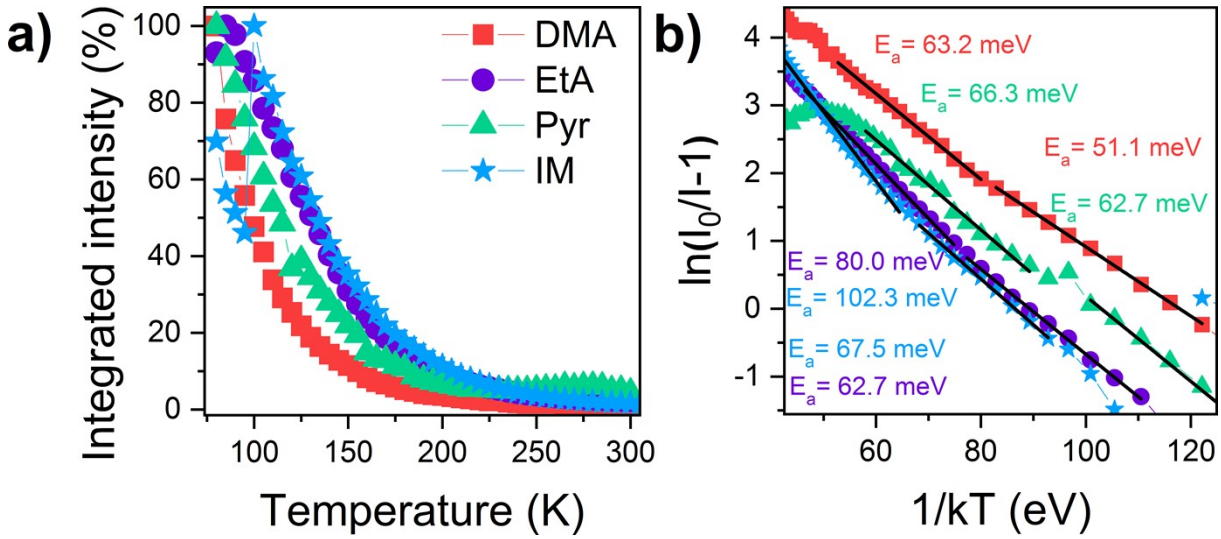

Figure S7. Changes of the PL integrated intensity of the investigated compounds with increasing temperature (a) and the energy activation (E_a) of thermal quenching (b).